SYMPLECTIC CELLULAR AUTOMATA

Kunihiko KANEKO
Institute of Physics, College of Arts and Sciences, University of Tokyo, Tokyo 153, Japan

Received 22 October 1986; accepted for publication 27 April 1987 [1]
Communicated by A.R. Bishop

Cellular automata (CA) corresponding to hamiltonian mappings are proposed. The features of such CA are classified into the linear wave, superposed complex, and ergodic-like. It is shown that most nontrivial symplectic CA show the ergodic behavior. Spatio-temporal patterns, Poincaré's recurrence time, spatial entropies and Poincaré maps are calculated to confirm the ergodicity for the check of "ergodicity". The variational principle for actions is discussed.

1. Introduction and models

Spatially extended dynamical systems with discrete time and space have recently been investigated extensively. For dissipative systems, coupled map lattices [1,3] and cellular automata (CA) [3,4] are typical models for the spatio-temporal complexity. Although hamiltonian systems with a large number of degrees of freedom should be investigated from the viewpoint of the origin of ergodicity and the foundation of statistical mechanics, the available discrete models are still few [5,6]. In the case of hamiltonian systems, we have to be careful in the model-making, since the mapping must obey the symplectic condition. Let us consider an N-particle hamiltonian system on a one-dimensional lattice with periodic boundary condition. The dynamics of the system is represented by a set of $2N$ variables $x(i)$ (displacement) and $p(i)$ (momentum) with $i=1, 2, \ldots, N$. Furthermore we use the discrete time dynamics, as can be widely used in the study of standard mapping by Chirikov and Taylor [5]. Then the model can be written as

$$x_{n+1}(i)=x_n(i)+p_{n+1}(i)\,,$$

$$p_{n+1}(i)=p_n(i)+F^i(\{x_n(j)\})\,, \tag{1}$$

where F^i is the force term for the ith particle, which depends on the displacements. i denotes the lattice site ($i=1, 2, \ldots, N$) and the suffix n is a discrete time. The mapping can be regarded as the Poincaré map of some $(N+2)$-dimensional hamiltonian system on an energy surface as is sometimes seen in the interpretation of the standard mapping [5], or more directly it is derived from the following hamiltonian with a delta-function force at the integer times:

$$H=\tfrac{1}{2}\sum_{i=1}^{N} p(i)^2+V(\{x(i)\})\sum_{n=-\infty}^{\infty}\delta(t-n)\,, \tag{2}$$

with the potential $V(x)$ such that

$$F^i(\{x(j)\})=-\frac{\partial V(\{x(j)\})}{\partial x(i)}\,.$$

The existence of the potential is guaranteed by the symplectic condition

$$\sum \mathrm{d}x_{n+1}(i)\wedge \mathrm{d}p_{n+1}(i)=\sum \mathrm{d}x_n(i)\wedge \mathrm{d}p_n(i)\,,$$

which imposes the following restriction on the force term

$$\frac{\partial F^i(\{x(k)\})}{\partial x(j)}=\frac{\partial F^j(\{x(k)\})}{\partial x(i)}\,. \tag{3}$$

The numerical studies for the class of models with the above condition have been and will be reported

[1] After acceptance, the manuscript had been lost in mail from the Editor to the Publisher. The Editor and the Publisher apologize for the delay caused by this accident.

0375-9601/88/$ 03.50

elsewhere [7–10]. Here we restrict ourselves to the one-dimensional lattice case with the nearest-neighbor coupling which depends only on the difference of the two sites. Then the symplectic condition is reduced to

$$F^i = K(x(i)) + G(x(i+1) - x(i)) + G(x(i-1) - x(i)) ,$$

$$G(x) = \text{odd function} . \quad (4)$$

Next, we discretize the state x. For this purpose we impose that $K(x)$ and $G(x)$ take only integer values for $x \in$ Integer. Then the dynamical variables x and p take only integers by the evolution (1), if we start from the integer initial conditions.

To obtain a CA with a finite number of states, we further impose the following condition: The force terms $K(x)$ and $G(x)$ are periodic functions with the period q, where the integer q is the number of the states in CA (let us regard, for example, that x is an angle variable). We further confine ourselves to the case with $q=3$ (i.e., $x = \pm 1, 0$), though the extension to arbitrary q is straightforward. Since the transformation $x(i) \to x(i) - 3$ does not change the dynamics for such system, our system is reduced to a CA with 3 states by the (mod) operation.

To sum up, the CA we simulate here is given by eqs.(1) with mod 3, and the force term with (4). The functions $G(z)$ and $K(z)$ and $K(z)$ ($z = \pm 1, 0$) are periodic functions with period 3 and take only the values ± 1 or 0. See fig. 1 for an example of $K(x)$ and the corresponding potential $U(x)$. Initially x and p take the values 1, −1, or 0.

Note that our CA is exactly governed by the hamiltonian

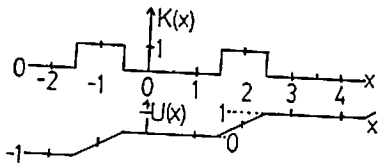

Fig. 1. Schematic representation of the force term $K(x)$ and the corresponding potential $U(x)$: $K(x)$ and $-U(x)$ are plotted for the rule $K(-1) = K(0) = 0$ and $K(1) = 1$.

$$H = \tfrac{1}{2} \sum_{i=1}^{N} p(i)^2 + \sum_{i=1}^{N} [K(x(i)) + L(x(i+1) - x(i))] \times \sum_{n=-\infty}^{\infty} \delta(t-n) ; \quad (5)$$

with

$$L(x) = -\partial G(x)/\partial x ,$$

and with the initial condition that $x(i)$ and $p(i)$ are 1, −1, or 0. Here we use the mod operation both for x and p. The mod operation for x is automatically satisfied by the condition for $G(x)$ and $K(x)$. The mod operation for p does not make any difference to the dynamics of x. In p-space, it is just a projection onto ± 1, 0 from integers. For the quantities we study later, the mod operation for p does not make any difference, though for some other quantities such as the kinetic energy $p^2/2$, we should make the simulation without mod operation for p.

The reason that we have not shown the results for the simplest case $q=2$ is that the system with $q=2$ always satisfies the superposition condition in a sense shown later and the behavior is essentially similar with the case with $q=3$ and with the superposition condition (see next section).

2. Classification and models

For $q=3$, the rules are classified by four numbers, i.e., $K(0)$, $K(1)$, $K(-1)$ and $G(1)$ (since $G(2) = G(-1) = -G(1) = 3 - G(1)$ and $G(0) = 0$). We can fix one of the K's, since the transformation $x \Rightarrow x \pm 1$ (mod 3) changes $K(x) \Rightarrow K(x) \pm 1$ (mod 3) with $G(x)$ unchanged. Here we fix $K(0) = 0$. Thus, we have 3^3 rules. Another transformation reduces the number of independent rules, i.e., the transformation $x \Rightarrow -x$ and $p \Rightarrow -p$ (mod 3). This transformation induces the change $K(0) \Rightarrow K(0)$, $K(1) \Leftrightarrow -K(-1)$, and $G(x) \Rightarrow G(x)$ (mod 3).

If the rule satisfies the condition

$$K(-1) - K(1) = K(1) - K(0) = K(0) - K(-1) \text{ (mod 3)} ,$$

the dynamics obeys the superposition condition, i.e.,

Table 1
Classification of the behavior of the symplectic CA with $q=3$. The model equation is written only for a reference, which has no serious meaning, where mod 3 must be taken.

K(−1)	K(1)	G(1)	Feature
arbitrary	arbitrary	0	trivial
0	0	1	linear wave [a]
1	−1	1	superposed complex [b]
−1	1	1	superposed complex [c]
1	0	±1	ergodic-like
1	1	±1	ergodic-like
−1	0	±1	ergodic-like

[a] The rule $(K(-1), K(1), G(1)) = (1, -1, -1)$ is obtained by the ferro–antiferro transformation from this rule for even N. For odd N, this transformation can give a slight change; e.g., the PRT is twice.

[b] The rule $(-1, 1, -1)$ is obtained by the above transformation, for even N.

[c] The rule $(0, 0, -1)$ is obtained by the above transformation, for even N.

$$x_n(i) = x_n^{(1)}(i) + x_n^{(2)}(i) \text{ (mod 3)}$$

if

$$x_0(i) = x_0^{(1)}(i) + x_0^{(2)}(i) \text{ (mod 3)}$$

(same for $p(i)$). If the rule satisfies the superposition condition, the ferro–antiferro transformation [11] gives another class of equivalence among the rules. That is, the transformation

$$x(2i), p(2i) \Leftrightarrow -x(2i), -p(2i)$$

(for $i = 1, 2, \ldots, N/2$) induces the change

$$G(x) \Leftrightarrow -G(x)$$

and

$$K(x) \Leftrightarrow K(x) - x \text{ (mod 3)} .$$

Thus, the dynamics for the rule with the superposition condition and $G(1) = -1$ is simulated by the rule with $\bar{K}(x) = K(x) + x$ and $G(1) = 1$, through the change $x(2i) \Rightarrow -x(2i)$ and $p(2i) \Rightarrow -p(2i)$. (For odd N, this transformation induces a change of the boundary condition, and makes a slight change of behavior, which is not essential for large N.) Thus, the independent rules are reduced to those in the list shown in table 1. We have numerically investigated these rules, which can be classified into the following four cases, the first three of which satisfy the superposition condition.

(I) Non-coupling ($G(1) = 0$). Of course, this case is trivial, since the state of a site is independent of neighbors' sites. In the following we treat only the non-trivial case, i.e., $G(1) \neq 0$.

(II) Linear-wave motion ($K(0) = K(1) = K(-1)$, and $G(1) = 1$)). The force term is independent of the value of the self-site at the previous step and the coupling interaction is the discretization of the linear force $G(x) = x$. The model can be regarded as the discretization of the model $\ddot{x} = \nabla^2 x$. The motion is characterized by the linear combination of the wavy propagation of the region with $x(i) \neq x(i+1)$ (see fig. 2).

(III) Superposed irregular motion ($K(1)K(-1) = -1$). Here again the rule satisfies the above superposition condition, but the dynamics gives a complicated behavior, in an analogous way to rule 90 in the dissipative CA (see ref. [3]). If we start from a single seed initial condition, the spatio-temporal pattern is characterized by the square structures of various sizes (see fig. 3).

(IV) "Ergodic-like" motion (for other rules). The pattern seems to be quite complicated and does not show any specular pattern for most initial conditions (see fig. 4). Since the dynamics of hamiltonian systems with large number of degrees of freedom is expected to show the ergodic behavior, we may term the above behavior as ergodic-like. The confirmation of the ergodicity is the topic of the next section.

3. Quantitative characterization

In order to study the complicated behavior in the non-trivial cases and to check the ergodicity, we have investigated the following quantities for the CA with size N.

3.1. Poincaré recurrence time

For a reversible CA with a finite size, the state returns to the initial state after some iterations. The time steps necessary for this recurrence may be called Poincaré recurrence time (PRT).

The PRT depends on the initial condition and in some case the distribution of PRT may also be important.

For class (II), the PRT is given by $3N$ except for

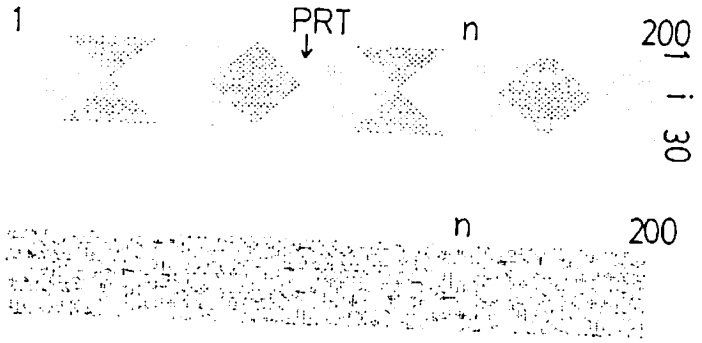

Fig. 2. Spatio-temporal pattern of the rule $K(1)=K(-1)=0$ and $G(1)=1$: (a) from single seed, (b) from random initial configurations. Size $N=30$; PRT is 90. In the following, the blank, +, and · show the region $x=0$, $x=-1$, and $x=1$, respectively.

Fig. 3. Spatio-temporal pattern of the rule $K(1)=1$, $K(-1)=-1$, and $G(1)=1$ from a single seed. Size $N=30$. The PRT is 760.

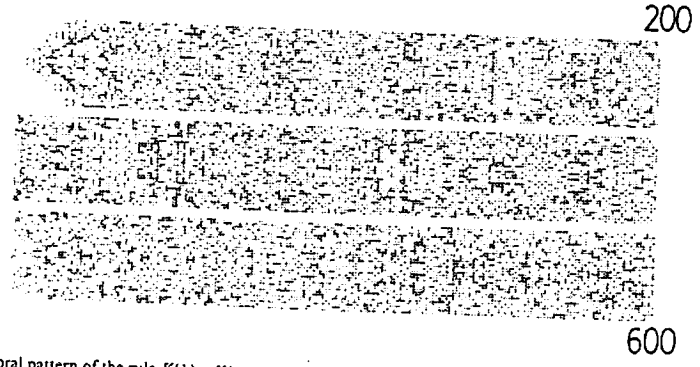

Fig. 4. Spatio-temporal pattern of the rule $K(1)=K(-1)=1$ and $G(1)=1$ from a single seed. Size $N=30$. At the time step $T=600$, the recurrence has not yet occurred.

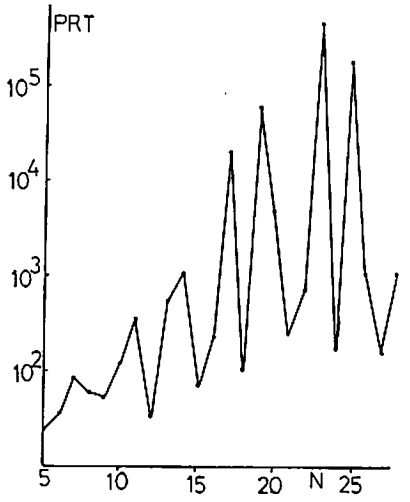

Fig. 5. PRT as a function of size N for the rule $K(1)=1$, $K(-1)=-1$, and $G(1)=1$.

the trivial initial condition (e.g., $x(i)=0$ for all i) as is easily shown.

For class (III), the PRT shows a quite complicated behavior with size N. Since the superposition

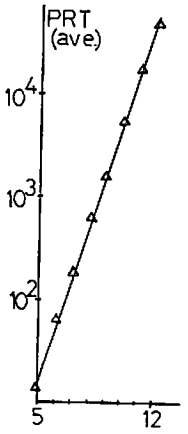

Fig. 6. Average PRT as a function of size N for the rule $K(1)=0$, $K(-1)=1$, and $G(1)=1$. The average is calculated from randomly chosen 500 initial configurations.

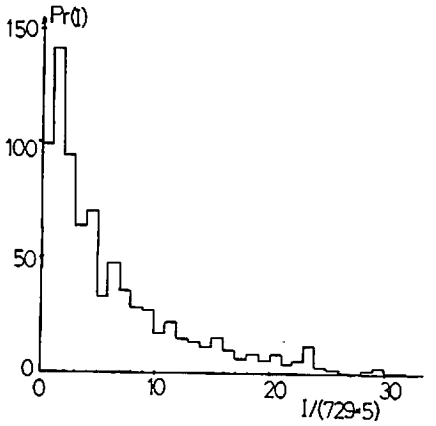

Fig. 7. Histogram of the distribution of PRT for the rule $K(1)=0$, $K(-1)=-1$ and $G(1)=1$. $N=9$. Random 800 initial configurations are chosen. Longitudinal axis is the number of initial configurations which give $3^n\times 5i < PRT < 3^n\times 5(i+1)$ for $i=1, 2, \ldots, 30$.

is valid, the PRTs for arbitrary states is given from the PRTs for the single seed initial conditions. In fig. 5, the longest PRT as a function of size is plotted. The increase is quite slow and depends on the number-theoretical character of the size N, which is analogous to the case in rule 90 in dissipative CA.

For class (IV), the PRT increases exponentially with size. The increase is roughly fitted by α^N (fig. 6), though there can be a difference by the parity of the size N for some rules. The number α scatters around ~3.0–5.0, which slightly depends on the rule. The PRT distributes rather broadly (see fig. 7).

If the phase space were covered by a few number ($o(N)$) of orbits, the PRT would grow as 9^N. In the present case, there still exist orbits with the number of $O(\beta^N)$, with $\beta \sim 9/\alpha$. In this sense, our system does not obey the ergodicity in the narrowest sense that a single orbit covers the whole phase space.

3.2. Local recurrence time

Let us take a small subsystem (size M) within a system. If the statistical mechanics is valid for a class (IV) system, the residual system may be regarded as

the heat bath for the region M. Here we study the recurrence time only for the local region M. We calculate the time I necessary for $x_I(i)=x_0(i)$ and $p_I(i)=p_0(i)$ for $i=1, 2, ..., M$ for various states, to get the distribution function $\Pr(I)$ of the local recurrence time. As is shown in fig. 8, the distribution function $\Pr(I)$ for the local recurrence time I is fitted by the distribution $\Pr(I)=\exp(-I/T_M)$ where $T_M=9^M$ if N is large enough. If the variables x and p can take each of the 3 values ±1, 0 randomly ($9=3^2$), the above distribution is expected. This is the first illustration of the local ergodicity. The residual system acts as a heat bath. If the system size N is not large enough compared with the local system size M, the local recurrence time is much smaller. It increases with system size N, till it saturates at some size N (which is rather small $\lesssim 4M$). Thus, the local equilibrium is attained within a smaller time scale ($o(N)$) than PRT.

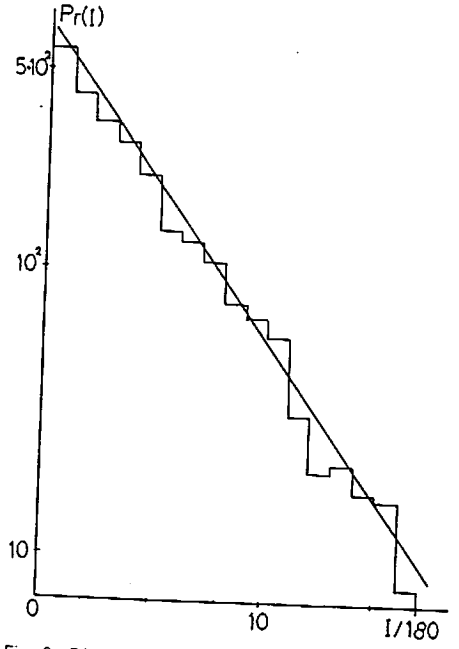

Fig. 8. Distribution of local PRT for the rule $K(1)=0$, $K(-1)=-1$ and $G(1)=1$: $N=50$ and $M=3$. Single seed initial condition. Long time sampling (sample number=2500) is taken after discarding initial 1000 steps. Longitudinal axis is the number of events such that $180\times i<$ local PRT $<180\times(i+1)$ for $i=1, ..., 17$. The line shows $\exp(-I/9^M)$.

3.3. Entropies [3,4]

We have investigated the s-character entropies for the spatial sequence of (x, p), i.e.,

$$S=-\sum P(x_1, p_1, x_2, p_2, ..., x_s, p_s) \times \log P(x_1, p_1, x_2, p_2, ..., x_s, p_s)/\log 3^{2s}, \quad (6)$$

or the s-character entropies for the spatial sequence of x only, i.e.,

$$S_x=-\sum \bar{P}(x_1, x_2, ..., x_s) \times \log \bar{P}(x_1, x_2, ..., x_s)/\log 3^s, \quad (7)$$

where P and $\bar{P}$ are the probabilities of the occurrence of such symbol sequences.

We have made simulations for $s<6$ for (6) and $s<9$ for (7), for the rules of classes (III) and (IV). Both the entropies take unity within 1% (we have checked for $N=200$). Thus, the possible state of the small subsystem (lattice size s) has an equal probability (equipartition). This means that our system satisfies the condition for the statistical mechanics.

3.4. Poincaré plots a la Grassberger [12]

Another method of visualization is the two-dimensional plot for the number of (X_n, P_n), where

$$X_n=\sum x_n(i)/3^i, \quad P_n=\sum p_n(i)/3^i. \quad (8)$$

For most irreversible CA with triangle patterns and some reversible CA, the Cantor set structure is remarkably seen [12,19]. In class (IV) models in our system, however, we cannot see any structure in the phase space. It seems that the orbits (X_n, P_n) travel any neighborhood of the points in the phase space (X, P) if the system size is large. This feature is another manifestation of the "ergodicity" (fig. 9).

4. Discussion and future problems

In the present Letter we have introduced a simple cellular automaton model, which is a discretization of a symplectic map lattice.

In the hamiltonian system, the variational principle about actions is useful [13]. In our system it is formulated as follows: The orbit $x_n(i)$ from $\{x_0(i)\}$ to $\{x_m(i)\}$ is given by the extrenum of the action

$$S=\sum_{n=1}^{m}\sum_{i=1}^{N}\{\tfrac{1}{2}[x_n(i)-x_{n-1}(i)]^2 -\tfrac{1}{2}G(1)[x_n(i+1)-x_n(i)]^2-U(x_n(i))\}, \quad (9)$$

where $U(x)$ is the potential term corresponding to the force term $K(x)$ (see fig. 1). The variation here is taken over $\bar{x}_n(i)=x_n(i)+\delta x_n(i)$ with $\delta x_n(i)=\pm1$. Thus, the iterations of our CA are the process to choose an extremum state in the two-dimensional spin systems with q-states, i.e., the Potts model (see also ref [14]). Here, however, we have to be careful in the application of (mod q), since the potential term increases or decreases without bound and we cannot use the mod operation in the expression of the action. Thus, the state of x cannot be restricted to q-states in expression (9).

In quantum mechanics, the phase space is quantized by h^{3N}. In our system, the phase space is also quantized. By introducing the wave-function on our phase space we can simulate a many-body quantal system. The direction of this approach for the system with 1.5 degrees of freedom was originally performed by Hannay and Berry [15], in which case the quantization of Arnold's cat is related with the discrete state two-dimensional mapping, if some arithmetic condition is satisfied. A similar approach is possible to our system, which may give a tractable quantum mechanical model with many degrees of freedom [16]. The path integral formulation based on the above action principle will be useful for this study.

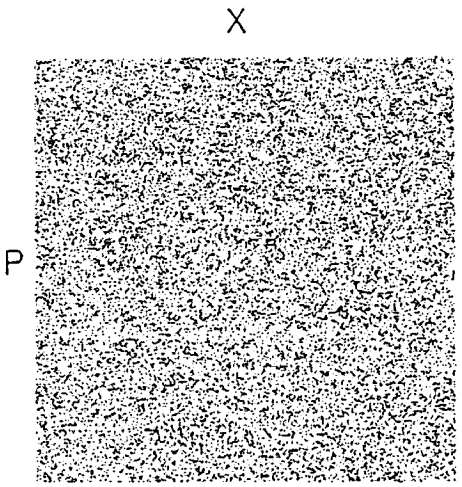

Fig. 9. Poincaré plots: (X_n, P_n) according to (6) are plotted for $n=1, 2, ..., 100000$. The rule is $K(1)=0$, $K(-1)=1$, and $G(1)=1$. Single seed initial condition.

There exist some other CA which can be related with hamiltonian dynamics. One example is the deterministic Ising model by Creutz [17], in which the energy is conserved (in our system it is not defined as is the case in the standard mapping [5]), but the dynamics itself is not governed by a hamiltonian. His model is of interest in connection with the phase transition and ergodicity. We can study the similar problem in a two-dimensional version of our symplectic CA.

In the case of two-variable area-preserving mappings, the discretization of states was performed previously by several authors [15,19]. If we increase the number of states q, our model is an extension of these studies to a large number of degrees of freedom. In the case of dissipative coupled map lattices, the relation to CA by this kind of discretization is discussed [18]. The similar studies in the hamiltonian systems will be of use in the future [*1].

Another unresolved question is the difference in the behavior between our symplectic CA and the reversible CA [20]. In the case of the two-state CA, the difference is clear, since we do not have nontrivial symplectic CA, while in the reversible CA with the range 3, we have a lot of nontrivial ones. In the general case, however, we are not sure what restriction is imposed on the global behavior by the symplectic condition.

The author would like to thank Drs. S. Takesue, T. Konishi, Y. Iba, and S. Adachi for useful discussions and critical comments. He would also like to thank the Institute of Plasma Physics at Nagoya for the facility of FACOM M200 and VP200. This work

[*1] While writing the manuscript, I was informed of the preprints by I. Percival and F. Vivaldi, in which a discrete state dynamics corresponding to the cat map is investigated.

was partially carried out under the ISM Cooperative Research Program and was partially supported by the Scientific Research Fund of the Ministry of Education, Science and Culture.

References

[1] K. Kaneko, Ph.D. thesis (1983) [Enlarged version: Collapse of tori and genesis of chaos in dissipative systems (World Scientific, Singapore, 1986)]; Progr. Theor. Phys. 72 (1982) 480; 74 (1985) 1033;
R.J. Deissler, Phys. Lett. A 100 (1984) 451;
I. Waller and R. Kapral, Phys. Rev. A 30 (1984) 2047;
J.D. Keeler and J.D. Farmer, Physica D 23 (1986) 413;
K. Kaneko, Physica D 23 (1986) 436.
[2] J.P. Crutchfield and K. Kaneko, in preparation.
[3] S. Wolfram, Rev. Mod. Phys. 55 (1983) 601; Physica D 10 (1984) 1.
[4] S. Wolfram, ed., Theory and applications of CA (World Scientific, Singapore, 1986).
[5] B.V. Chirikov, Phys. Rep. 52 (1979);
A.J. Lichtenberg and M.A. Lieberman, Regular and stochastic motion (Springer, Berlin, 1983).
[6] F. Vivaldi, Rev. Mod. Phys. 54 (1984) 737.
[7] C. Froeschle, Astron. Astrophys. 16 (1972) 172;
K. Kaneko and R.J. Bagley, Phys. Lett. A 110 (1985) 435.
[8] K. Kaneko, Proc. US–Japan Workshop on Statistical plasma physics, IPP-report (1986); and in preparation.
[9] G. Paladin and A. Vulpiani, Phys. Lett. A 118 (1986) 14.
[10] R. Hirota, J. Phys. Soc. Japan 50 (1981) 3785;
T. Konishi, in preparation.
[11] K. Kaneko and Y. Akutsu, J. Phys. A 19 (1986) L69.
[12] P. Grassberger, Physica D 10 (1984) 52.
[13] J.M. Greene, J. Math. Phys. 20 (1979) 1183;
D. Bensimon and L.P. Kadanoff, Physica D 10 (1984) 82;
R.S. Mackay, J.D. Meiss and I.C. Percival, Physica D 13 (1984) 55.
[14] E. Domany and W. Kinzel, Phys. Rev. Lett. 53 (1984) 311.
[15] J.H. Hannay and M.V. Berry, Physica D 1 (1980) 267.
[16] S. Adachi, private communication.
[17] M. Cruetz, Ann. Phys. 167 (1986) 62.
[18] J.P. Crutchfield and N.H. Packard, private communication; Int. J. Theor. Phys. 21 (1983) 433;
K. Kaneko, Collapse of tori and genesis of chaos in dissipative systems (World Scientific, Singapore, 1986) p. 243;
I. Shimada, private communication.
[19] F. Rannou, Astron. Astrophys. 31 (1974) 289.
[20] Y. Pomeau, J. Phys. A 17 (1984) 415;
S. Takesue, to be published.